



## Nuclear Orientation of Radon Isotopes by Spin Exchange Optical Pumping

M. Kitano\*, F. P. Calaprice, M. L. Pitt  
J. Clayhold, W. Happer, M. Kadar-Kallen, M. Musolf  
*Department of Physics, Princeton University, Princeton, New Jersey 08544*

G. Ulm† K. Wendt‡  
*ISOLDE, CERN, Geneva, Switzerland*

T. Chupp  
*Harvard University, Cambridge, Massachusetts 02138*

J. Bonn, R. Neugart, E. Otten  
*Universität Mainz, Mainz, Germany*

and  
H. T. Duong  
*Laboratoire Aimé Cotton, Orsay, France*

and the ISOLDE Collaboration

subm. to Phys. Rev. Lett.

June, 1987

### Abstract

This paper reports the first demonstration of nuclear orientation of radon atoms. The method employed was spin exchange with potassium atoms polarized by optical pumping. The radon isotopes were produced at the ISOLDE isotope separator of CERN. The nuclear alignment of  $^{209}\text{Rn}$  and  $^{223}\text{Rn}$  has been measured by observing  $\gamma$ -ray anisotropies and the magnetic dipole moment for  $^{209}\text{Rn}$  has been measured by the nuclear-magnetic-resonance (NMR) method to be  $|\mu| = 0.83881(39)\mu_N$ .

\*Present address: Radio Atmospheric Science Center, Kyoto University, Uji 611, Japan.

†Present address: Physikalisch-Technische Bundesanstalt Institut Berlin, Berlin, Germany

‡Present address: Universität Mainz, Mainz, Germany

Nuclear polarization methods have been very useful for studies of nuclear structure and for investigations of fundamental nuclear processes. For example, the polarization of noble gas atoms has been especially useful for studies of time reversal invariance [1] and nuclear electric dipole moments (EDM) [2]. This special feature of the noble gas atoms is due to the long spin depolarization times. One might also expect that polarized radon atoms would be very useful for such studies, and in particular for measurements of nuclear EDM [3], because atomic electron screening effects are reduced as the atomic number increases and an enhancement of nuclear EDM by state mixing is expected for some radon isotopes. But to date no method has been available for producing nuclear orientation of gaseous radon.

We report here the first demonstration of nuclear orientation of radon. The radon nuclei are oriented by spin exchange collisions with alkali atoms that are polarized by optical pumping. This method has been employed previously to polarize the lighter noble gas atoms and most extensively xenon for which polarizations of  $\gtrsim 70\%$  are readily achieved [4,5,8].

The cross-section for spin exchange is larger for the heavier noble gas atoms, owing, in part, to the importance of the formation of alkali-noble gas atom molecules [6,7]. For this reason we expected that radon would be readily polarized by spin exchange on alkali atoms too. A detailed discussion of the spin-exchange process is given in [8].

On the other hand, for radon we anticipated significantly larger depolarization due to the wall sticking compared to xenon. So special attention has been paid to reduce the quadrupole relaxation on the cell wall as described later.

As in earlier studies of radioactive xenon isotopes [4,5], we have used the  $\gamma$ -ray anisotropy method to observe the nuclear orientation. We chose  $^{209}\text{Rn}$  (half life  $t_{1/2} = 29$  min) for these studies as it has a reasonably well established decay scheme, enabling us to predict the expected  $\gamma$ -ray anisotropy, and because its hyperfine

structure has recently been studied by collinear laser spectroscopy [9]. The laser spectroscopy has also established the spin  $I = 5/2$  by direct measurement and a positive sign of the magnetic moment of  $^{209}\text{Rn}$ . Our direct measurement of the magnetic moment would provide a calibration of the hyperfine magnetic field of the radon atom.

We also polarized  $^{223}\text{Rn}$  ( $t_{1/2} = 23$  min, [12]) by the spin exchange method and the  $\gamma$ -ray anisotropies of several  $\gamma$  transitions have been measured. The decay scheme of this isotope has not been established yet but a preliminary study of the  $\gamma$ -ray lines and multiplicities has been published [12].

The radon activity was produced at the ISOLDE isotope separator facility of CERN by spallation reaction of 600 MeV protons on a  $55 \text{ g/cm}^2$   $\text{ThC}_2$  target. Previous studies [10] demonstrated high radon yields with  $1.5 \times 10^8$   $^{209}\text{Rn}$  atoms per sec per microamp of beam. With this flux we were able to obtain sufficiently strong samples ( $10 \mu\text{Ci}$ ) of  $^{209}\text{Rn}$  with collection times of about 10 sec.

The optical pumping cells were filled with radon isotopes with the apparatus illustrated in Fig. 1a. The mass separated 60 keV  $\text{Rn}^+$  was stopped in a thin ( $7.6 \mu\text{m}$ ) tantalum foil within a small target chamber evacuated to pressures of  $\sim 10^{-7}$  torr. The target chamber has lines to gas bottles containing  $\text{H}_2$  and  $\text{N}_2$ , a sidearm containing potassium as a getter, and a port to valve V4 on which the cell glassware is attached.

In advance of the run, we prepared several pyrex glass cells (1 cm diameter) loaded with a few mg of potassium and  $\sim 5$  torr of  $\text{H}_2$  gas. Potassium was used as the alkali for spin exchange, rather than rubidium as in past xenon experiments [4,5], to permit operation of the cells at a high temperature ( $250^\circ\text{C}$  instead of  $190^\circ\text{C}$ ) and thereby reduce depolarization of radon by wall sticking. The  $\text{H}_2$  was introduced and the cells were heated for a few days at  $80^\circ\text{C}$  to form a surface layer of potassium hydride which also reduces wall relaxation [11].

After the implantation, the Rn beam is turned off and valves to the chamber are

closed. The Ta foil is heated to a bright whitish-orange glow by passing a current of 20 A through it for 2 min. Valve V4 is opened allowing the getter to remove any gas that may have leaked into the glass tube to the cell. The glass sidearm is now cooled with liquid nitrogen condensing the radon in the smaller volume beyond valve V4. Valve V4 is now closed and the sidearm is warmed, the cell breakseal is opened with a magnetic hammer, and the cell is cooled with liquid nitrogen, moving the radon into the cell. Valve V4 is now opened to introduce 400 torr of N<sub>2</sub> and 10 torr of H<sub>2</sub> and then closed. Finally, the cell is pulled off with a torch while cooling the bottom of the cell with liquid nitrogen.

The cell containing radon is placed in an oven and heated by flowing hot air to about 230 °C (see Fig. 1b). A krypton ion laser (Coherent K3000) and a dye laser (Coherent CR699), operating in standing-wave mode with LD700 dye, produces 0.8 W of light at the 769.9 nm *D*<sub>1</sub> line of potassium at the cell. The light is right- or left-circularly polarized with a  $\lambda/4$  plate placed just in front of the cell. A few gauss of magnetic field parallel to the light beam is produced by a single pair of Helmholtz coils and a power supply stable to  $1/10^4$ .

The nuclear alignment of the radon was monitored by observing the  $\gamma$ -ray anisotropy between two IGe detectors (12 %, Ortec) placed at 0° and 90° relative to the magnetic field. The  $\gamma$ -ray spectra were acquired for typically 5 min intervals with a two channel CAMAC analog-to-digital converter and histogramming memory system that was interfaced to an Apple IIe microcomputer. An acquisition program was used to calculate  $\gamma$  anisotropies on-line.

The  $\gamma$ -ray spectrum for <sup>209</sup>Rn in the vicinity of the 745 keV line is illustrated in Fig. 2. A simplified decay scheme of <sup>209</sup>Rn, illustrating some of the prominent  $\gamma$ -ray transitions is also shown in Fig. 2. The anisotropy ratios *R* for the strong  $\gamma$ -ray transitions are given in Table I. The quantity *R* computed is the ratio of counts in the 0° detector to counts in the 90° detector for laser on divided by the same for laser off. That is,  $R = r(\text{laser on})/r(\text{laser off})$ , where  $r = \text{Counts}(0^\circ)/\text{Counts}(90^\circ)$ .

From these results we see that the  $^{209}\text{Rn}$  is definitely aligned. The anisotropy of the 745 keV line is predicted to be 1.3 assuming it is a pure M1 transition and that the spin for the 745 keV level is  $7/2$  and that all initial  $^{209}\text{Rn}$  nuclei with spin  $5/2$  are in the  $m = +5/2$  magnetic substate. The observed anisotropy indicates that the alignment is about 50 % of the maximum possible alignment.

To observe nuclear alignment of  $^{223}\text{Rn}$ , a cell containing  $^{223}\text{Rn}$  was prepared in the same way as described above for the  $^{209}\text{Rn}$  cell. The anisotropies for prominent  $\gamma$ -ray lines are given in Table II. Several of the  $\gamma$ -ray lines exhibit a significant anisotropy. These results should be useful in combination with other studies of the decay scheme of  $^{223}\text{Rn}$  to produce a level diagram with definite spin parity assignments. There are many other  $\gamma$ -ray lines in this decay. A complete analysis of  $^{223}\text{Rn}$   $\gamma$  anisotropies and the  $\gamma$ -anisotropies of  $^{209}\text{Rn}$  will be presented in a future publication.

The magnetic moment of  $^{209}\text{Rn}$  was measured by searching for a resonant destruction of the nuclear alignment with application of a transverse oscillating magnetic field of variable frequency. The resonance curve is shown in Fig. 3. The amplitude of the oscillating field was increased to produce a resonance width of several Hz to facilitate the search.

To obtain the magnetic dipole moment from the resonance frequency we need to determine the magnetic field. The field was measured by observing the  $^{129}\text{Xe}^m$  ( $t_{1/2} = 8.89$  day) NMR resonance in a similar cell that was filled with the ISOLDE facility. The magnetic moment of  $^{129}\text{Xe}^m$  is accurately known [4,5]. However, it is important to realize that there are two sources of the magnetic field that the noble gas atoms experience: (1) the externally applied field  $B_0$  and (2) a field  $B_{\text{coll}}$  due to the spin exchange process with the polarized alkali vapor [6]. Furthermore,  $B_{\text{coll}}$  depends on the particular rare gas atom and must be measured separately for each case. Therefore, we have measured the NMR resonances for the radon and calibration xenon isotopes with both polarizations of the light,  $\sigma_+$  and  $\sigma_-$ , or

equivalently both polarizations of the alkali vapor, but with the same external field direction in both cases (See Fig. 1b). From the four frequencies thus measured and the magnetic moment of  $^{129}\text{Xe}^m$ , we can derive  $B_0$ ,  $B_{\text{coll}}^{(\text{Xe})}$ ,  $B_{\text{coll}}^{(\text{Rn})}$ , and the magnetic moment of  $^{209}\text{Rn}$ .

The NMR frequencies  $\nu_{\pm}$  of  $^{209}\text{Rn}$  and  $^{129}\text{Xe}^m$  for the  $\sigma_{\pm}$  pumping are given in Table III along with related quantities. The magnetic moment of the  $^{129}\text{Xe}^m$  given in Table III has been corrected for diamagnetism. Likewise the magnetic moment for  $^{209}\text{Rn}$  derived from it is corrected for diamagnetism by means of the following equation:

$$|\mu^{(\text{Rn})}| = |\mu^{(\text{Xe})}| \frac{(\nu_{+}^{(\text{Rn})} + \nu_{-}^{(\text{Rn})}) I^{(\text{Rn})} (1 - \sigma^{(\text{Xe})})}{(\nu_{+}^{(\text{Xe})} + \nu_{-}^{(\text{Xe})}) I^{(\text{Xe})} (1 - \sigma^{(\text{Rn})})},$$

where the spins  $I$  are 11/2 and 5/2 for  $^{129}\text{Xe}^m$  and  $^{209}\text{Rn}$ , respectively, and the diamagnetic corrections  $1/(1 - \sigma)$  are taken from [13].

In conclusion, the present work has demonstrated the feasibility of polarizing radon nuclei by the spin exchange optical pumping method. The spin transfer rate is apparently faster for radon than for xenon, as evidenced by the larger frequency shift  $\nu_{-} - \nu_{+}$  in Table III. In addition we have determined the magnetic moment of  $^{209}\text{Rn}$  by direct measurement. This result in combination with the measurement of the hyperfine structure of atomic transitions in  $^{209}\text{Rn}$  by collinear laser spectroscopy determines the magnetic hyperfine field (to be published), and, apart from hyperfine anomaly effects, also the magnetic moments of the other radon isotopes whose hyperfine structure has been measured [9]. Here we note that our value of the magnetic moment 0.83881 agrees fairly well with the estimate 0.82 given in [9]. The  $\gamma$  anisotropies of  $^{209}\text{Rn}$  and  $^{223}\text{Rn}$ , to be published, will aid in making spin-parity assignments of nuclear levels. Finally, the success of this work indicates that measurements of nuclear EDM of radon isotopes may be possible.

This work was performed with the ISOLDE collaboration. We thank Zhen Wu and Professor M. Morita for helpful discussions and Thad Walker for providing information on the Rb-Rn molecule. This work was supported by the National Sci-

entific Foundation, the U. S. Air Force Office of Scientific Research under Grant No. AFOSR 81-0104-C, and the German Federal Minister for Research and Technology (BMFT) under Contract No. 06 MZ 458 I.

## References

- [1] A. L. Hallin, F. P. Calaprice, D. W. MacArthur, L. E. Piilonen, M. B. Schneider and D. F. Schreiber, *Phys. Rev. Lett.* **52**, 337 (1984).
- [2] T. G. Vold, F. J. Raab, B. Heckel, and E. N. Forston, *Phys. Rev. Lett.* **52**, 2229 (1984).
- [3] V. V. Flambaum, I. B. Khriplovich, and O. P. Sushkov, *Phys. Lett.* **162B**, 213 (1985).
- [4] F. P. Calaprice, W. Happer, D. F. Schreiber, M. M. Lowry, E. Miron, and X. Zeng, *Phys. Rev. Lett.* **54**, 174 (1985).
- [5] M. Kitano, M. Bourzutschky, F. P. Calaprice, J. Clayhold, W. Happer, M. Musolf, *Phys. Rev. C* **34**, 1974 (1986).
- [6] B. C. Grover, *Phys. Rev. Lett.* **40**, 391 (1978).
- [7] C. H. Volk, T. M. Kwon, J. G. Mark, *Phys. Rev. A* **21**, 1549 (1980).
- [8] W. Happer, E. Mirron, S. Schaefer, D. Schreiber, W. A. van Wijngaarden, and X. Zeng, *Phys. Rev. A* **29** 3092 (1984), and references therein.
- [9] W. Borchers, R. Neugart, E. W. Otten, H. T. Duong, G. Ulm, K. Wendt, *Hyperfine Interact.* (in print).
- [10] F. Calaprice, G. T. Ewan, R. D. von Dincklage, B. Jonson, O. C. Jonsson, and H. L. Ravn, *Phys. Rev. C* **30**, 1671 (1984).
- [11] T. M. Kwon, J. G. Mark, and C. H. Volk, *Phys. Rev. A* **24**, 1894 (1981).
- [12] M. J. G. Borge, D. G. Burke, F. P. Calaprice, O. C. Jonsson, G. Lovhoiden, R. A. Nauman, K. Nybo, G. Nyman, H. L. Ravn, T. F. Thorsteinsen, *Zeit. f. Physik A* **325**, 429 (1986).



[13] *Table of Isotopes* edited by C. M. Lederer and V. S. Shirley (Wiley, New York, 1978).

## Tables

TABLE I. Summary of anisotropies for strong  $^{209}\text{At}$   $\gamma$  lines following  $^{209}\text{Rn}$  decay.

$E_\gamma$ (keV)	Spin Sequence	Anisotropy $R$	$R - 1$ (%)
337	$(7/2^-)-(5/2^-)$	0.903(14)	$-9.7 \pm 1.4$
408	$(5/2^-)-9/2^-$	1.009(7)	$+0.9 \pm 0.7$
689	$5/2, 7/2^- - 5/2^-$	1.079(22)	$+7.9 \pm 2.2$
745	$(7/2^-)-9/2^-$	1.129(14)	$+12.9 \pm 1.4$

TABLE II. Gamma ray anisotropies of  $^{223}\text{Fr}$  from the decay of oriented  $^{223}\text{Rn}$ .

$E_\gamma$ (keV)	Anisotropy $R$	$R - 1$ (%)
159.9	0.958(18)	$-4.2 \pm 1.8$
171.8	1.082(24)	$+8.2 \pm 2.4$
206.3	0.990(25)	$-1.0 \pm 2.5$
416.0	0.933(14)	$-6.7 \pm 1.4$
491.4	1.092(39)	$+9.2 \pm 3.9$
591.8	1.014(12)	$+1.4 \pm 1.2$
621.5	0.936(40)	$-6.4 \pm 4.0$
635.2	1.011(15)	$+1.1 \pm 1.5$
723.2	1.054(33)	$+5.4 \pm 3.3$

TABLE III. Frequencies of NMR resonances for  $^{209}\text{Rn}$  and  $^{129}\text{Xe}^m$  and related quantities.

	$^{129}\text{Xe}^m$	$^{209}\text{Rn}$
$I$	11/2	5/2
$\nu_+$ (Hz)	586.750(5)	1184.66(69)
$\nu_-$ (Hz)	588.292(60)	1218.77(32)
$\nu_- - \nu_+$ (Hz)	1.542	34.11
Collisional field $B_{\text{coll}}$ (G)	0.0063	0.067
External field $B_0$ (G)	4.790	
Diamagnetic correction <sup>a</sup> $1/(1 - \sigma)$	1.007092	1.0195
Magnetic Moment <sup>b</sup> $ \mu $ ( $\mu_N$ )	0.891223 <sup>c</sup>	0.83881(39)

a. Reference [13].

b. Corrected for diamagnetism.

c. Reference [5].

## Figure Captions

FIG. 1. The cell filling (a) and optical pumping (b) apparatus.

FIG. 2. The  $\gamma$ -ray spectrum of  $^{209}\text{At}$  following  $^{209}\text{Rn}$  decay. A simplified decay scheme of  $^{209}\text{Rn}$  is also shown.

FIG. 3. The NMR resonance curves for  $^{209}\text{Rn}$ . Count ratios between 745 keV and 337 keV lines for the  $0^\circ$  detector are plotted. As seen in Table I, these two lines show opposite sense of anisotropy. The two resonances correspond to the  $\sigma_\pm$  pumping (see text).

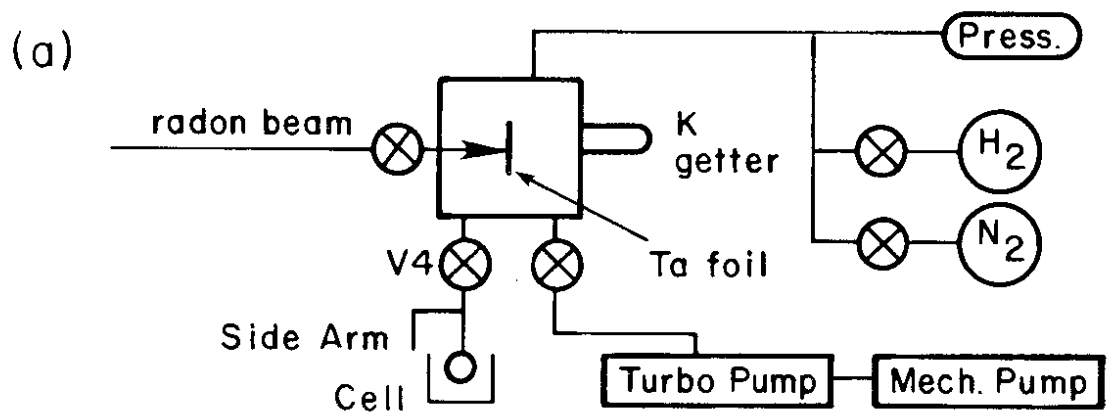
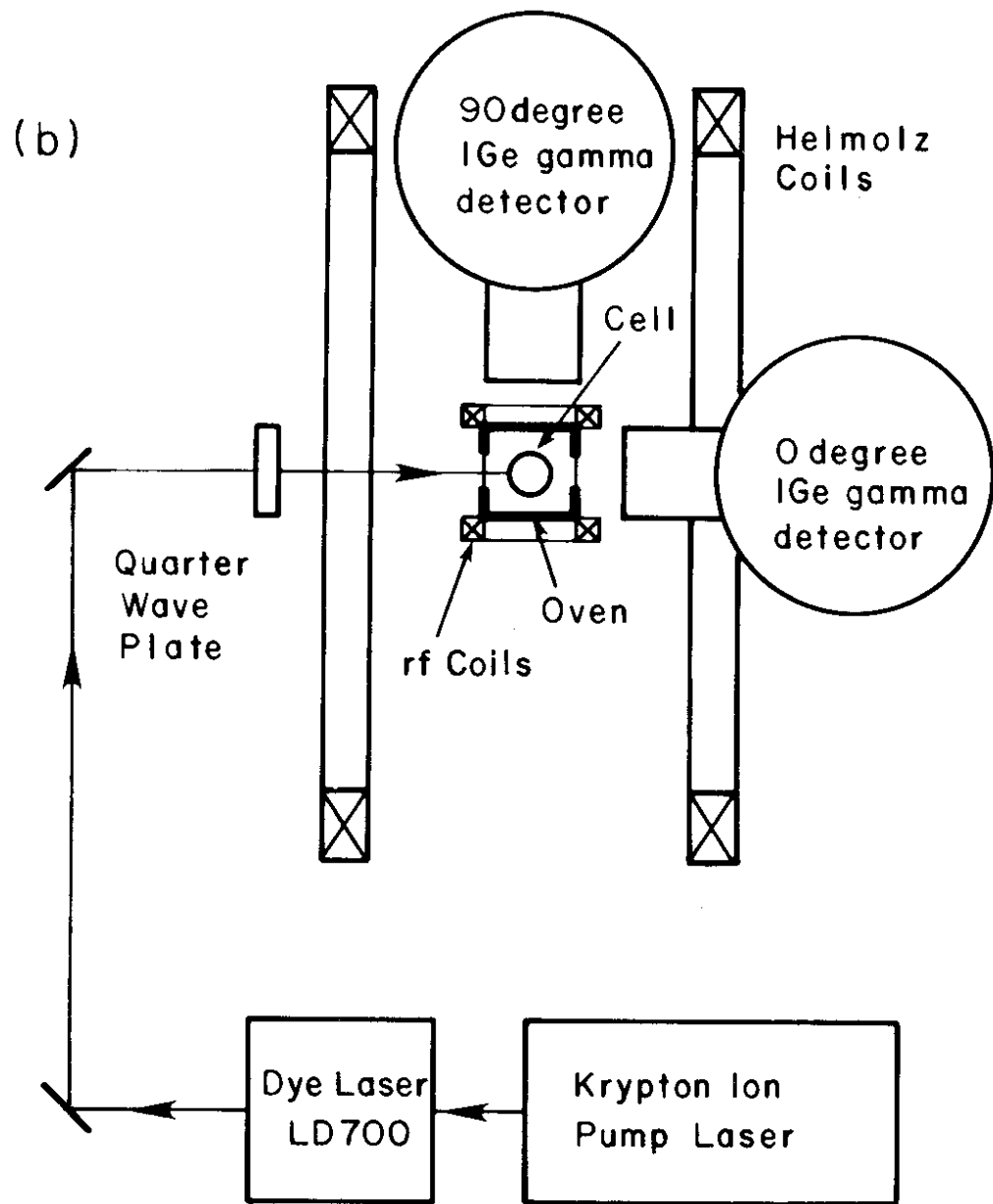


Fig. 1

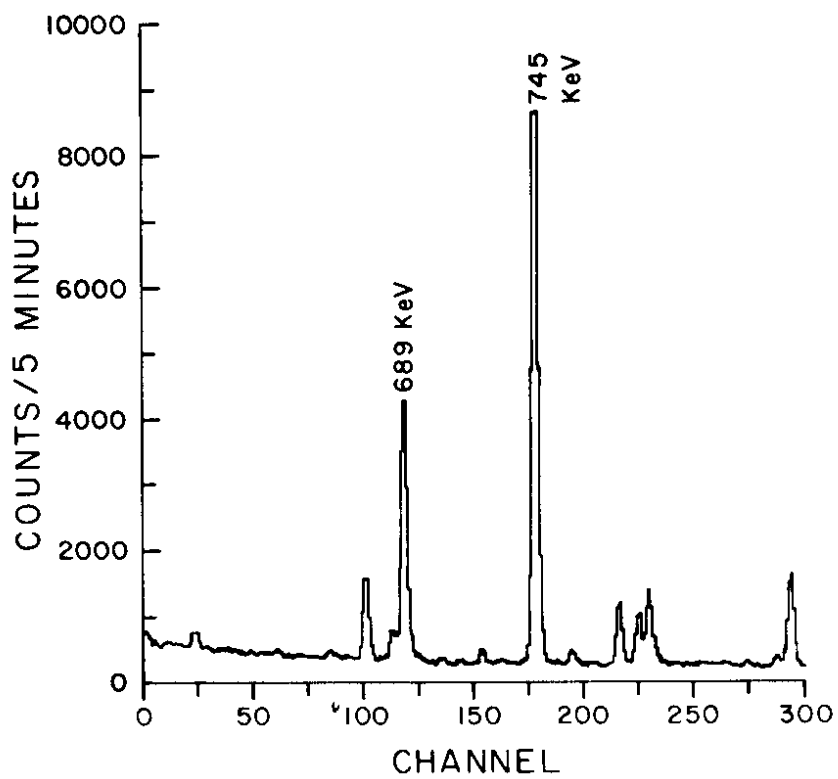
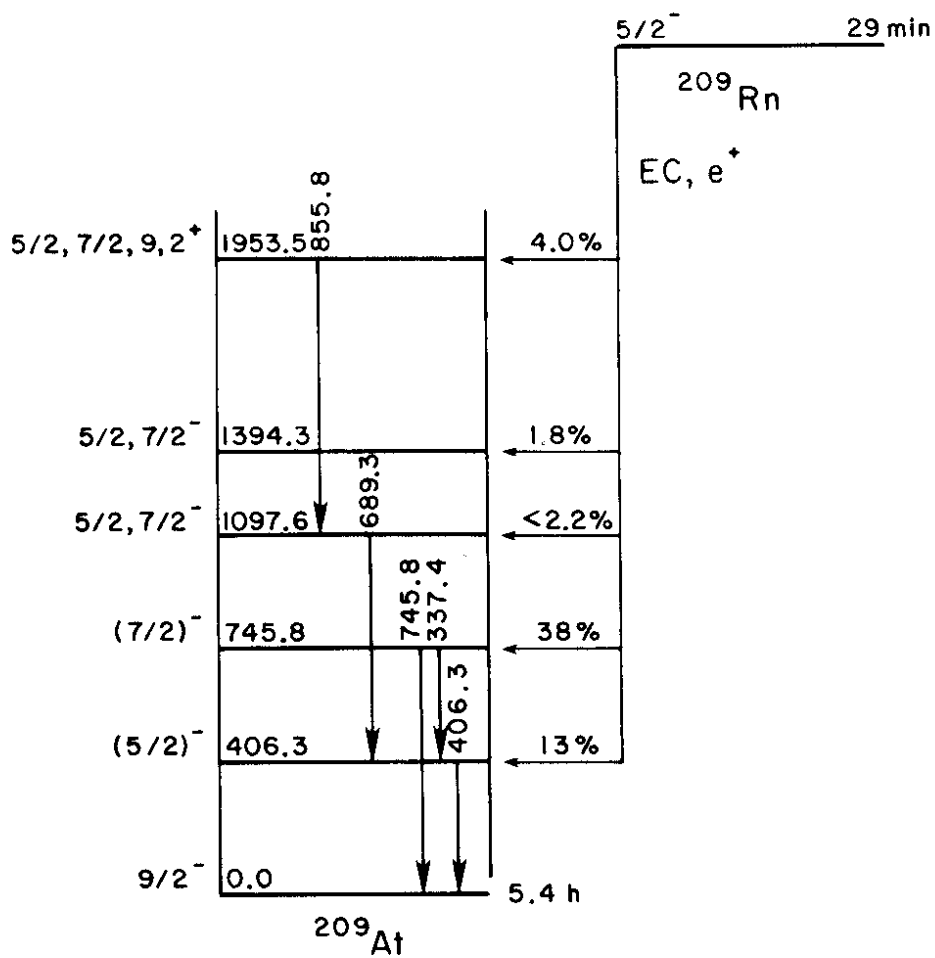


Fig. 2

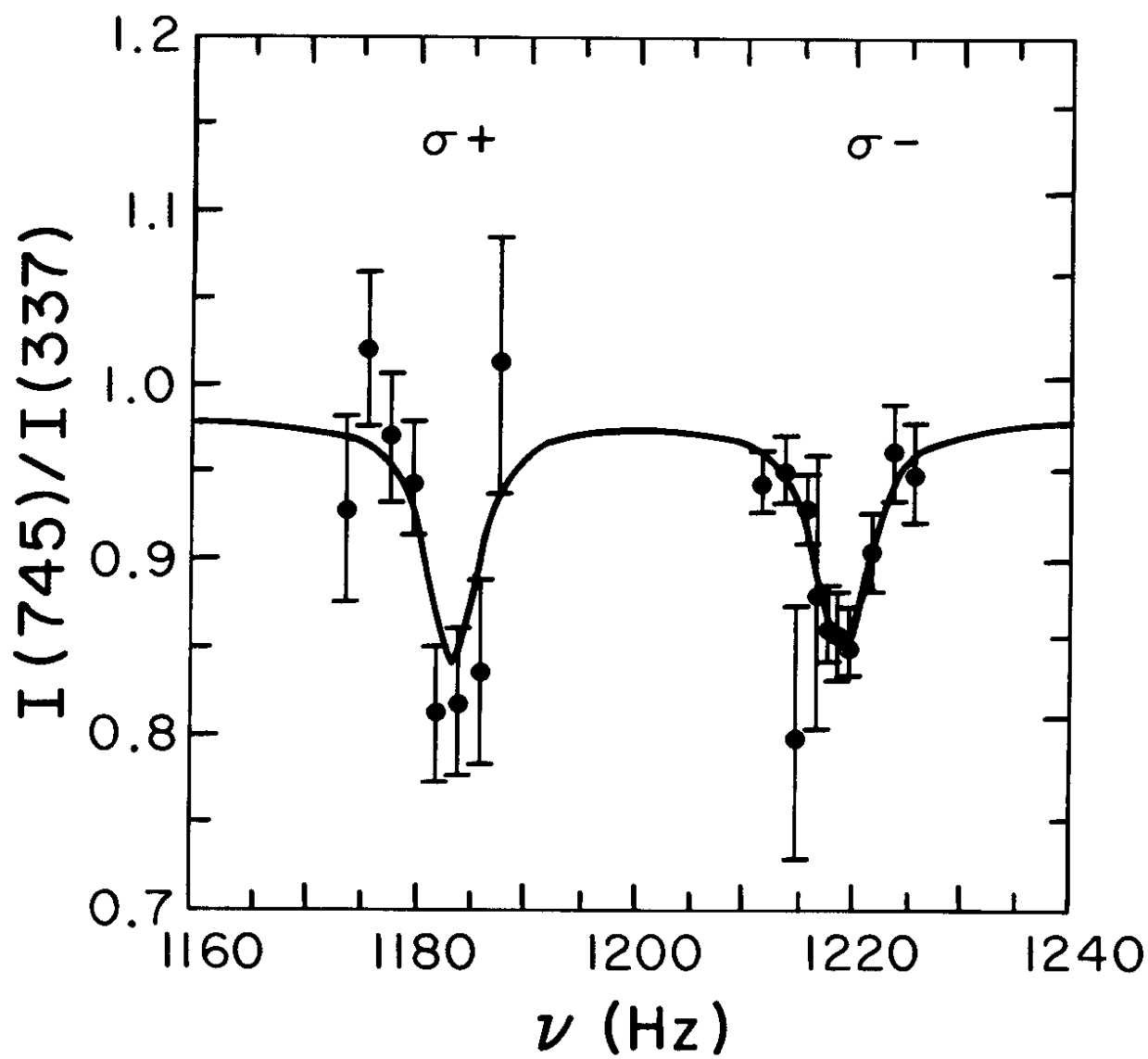


Fig. 3